Numerical Study on Thermophoretic Deposition of Highly Absorbing Emitting Particles Suspended in a Non-isothermal Two-Phase Flow System

비등온 이상유동 시스템에 부유된 고흡수, 방사하는 입자의 열환산적 부착현상에 대한 수치적 연구

S. J. Yoa* S. S. Kim**
여 석 준, 김 상 수

요 약

본 논문은 이상유동 시스템에 부유된 슈트, 미분탄과 같은 고 흡수, 방사하는 입자에 의한 열확산 현상에 대한 복사효과를 수치적으로 검토하였다. 가스, 입자유동의 지배방정식들은 오일러 관점의 two-fluid model 의 근간에서 수행되었으며, 에너지 방정식의 비선형 복사생성항은 P-1 근사방법에 의해 계산되었다. 복사효과가 증가될 때에 열확산적 입자의 벽면에 대한 부착율은 상당히 낮아짐을 보였으며 열확산 현상의 스토크스 수에 따른 효과도 고려되었다.

NOMENCLATURE

Glossary symbols

B_o	Boltzmann number (the ratio of the convection to radiation)
C_L	Thermal loading ratio
C_{pg}	Heat capacity of gas
C_{pp}	Heat capacity of particle
D	Tube diameter
D_p	Particle Brownian diffusivity
d_p	Particle diameter
E(x)	Cumulative collection efficiency
G_o	Dimensionless zeroth-order moment of intensity
I_b	Plank's black body function
K	Thermophoretic coefficient
K_g	Conductivity of the gas
K_p	Conductivity of the particle
N	The ratio of conduction to radiation
n_p	Number of particles per unit volume
Pe	RePr
Pr	Prandtl number
q_gR	Radiative heat flux for gas phase
q_pR	Radiative heat flux for particle phase
qR	Dimensionless radiative heat flux vector
R	Tube radius
Re	Reynolds number($=u_{avg}\ D/\upsilon$)
r	Radial coordinate
T	Temperature
u	Velocity in axial direction

* 한국과학기술원 기계공학과 대학원
** 정회원, 한국과학기술원 기계공학과

U_{avg}	Average velocity over the cross section in x-direction
v	Velocity in vector form in radial direction
v	Velocity in radial direction
V_T	Thermophoretic velocity
x	Axial coordinate

Greek character

α_T	Thermal diffusion factor
β	Absorption coefficient
ϵ_w	Wall surface emissivity
$\phi\Omega$	Azimuthal angle
ϕ	Dimensionless particle concentration ratio($\rho_p/\rho_{p,in}$)
η	Dimensionless radial coordinate
θ	Dimensionless temperature (T/T_{in})
θ_o	Dimensionless temperature at tube inlet(=1)
θ_m	Dimensionless mixed mean temperature (T_m/T_{in})
θ^*	$T_w/(T_{in}-T_w)$
$\theta\Omega$	Polar angle
ρ_g	Gas density
ρ_p	Apparent particle density
σ_g	Stress tensor of the gas
τ_A	Aerodynamic response time
τ_c	Mean time between particle-to-particle collision
τ_o	Dimensionless optical thickness
Ω	Solid angle
ξ	Dimensionless axial coordinate

Subscript

b	refers to black body
g	refers to gas phase
in	refers to tube inlet
max	refers to maximum
p	refers to particle phase
w	refers to wall surface

Superscript

R	refers to radiation
*	refers to dimensionless form

INTRODUCTION

Small particles such as dust, fly ash and soot suspended in a mixture system with a temperature gradient, experience a force in the direction opposite to the temperature gradient[1]. This so called thermophoresis phenomenon is therefore utilized in air cleaning device to remove submicron- and micron-sized particle from gas streams. The deposition of particulate material on heat exchanger surface with the concomitant reduction of exchanger effectiveness, particle deposition in automobile tailpipe, the fabrication of optical wave guide and semiconductor device have also been attributed to thermophoresis.

As investigated experimentally by Fulford et al.[2], Derjaguin et al.[3], Goldsmith [4], and S.S. Kim and Rosner[5], thermophoresis pheonomenon is important for particle diameter as large as 10μm and temperature gradient of the order of 50 K/cm(i.e propertional to -gradient(lnT) which produces the net thermophoretic transport). Moreover, in the presence of highly absorbing, emitting particles such as soot, fly-ash, and pulverized coal which significantly alter the temperature field of gas-solid mixture, the radiation effect on thermophoresis can be greatly important since the thermophoresis is strongly dependent upon the temperature gradient[6]. Up to the present, most of the experimental or numerical studies for the analysis of thermophoresis phenomenon has been carried out neglecting the radiation effect. Experimentally, thermophoretic deposition has been studied in laminar gas streams by Derjaguin et al.[3] for particles up to about 5 μm in diameter and Goldsmith et al.[4] for small particle, and in a turbulent pipe flow by Calvert and Byers[8]. Also, in the channel flows and boundary layer flows over a flat plate, the thermophoretic transport of particles has been studied analytically or

numerically by Goren[6], Epstein et al[9], etc and tube flow by Walker et al.[10]. Most of the workers for the analysis of thermophoresis mechanism have employed the low absorbing materials such as glass beads, TiO_2, MgO for particulate phase in two phase flow system. Particulary, Morse et al.[11] and Cipolla et al.[12] have considered the absorbing, non-emitting aerosol as long as the enclosure temperature is low when the particle is produced by laser heating in MCVD process. However, when the gas-solid mixture including soot, fly-ash and coal as undesirable byproducts is taken as a moving fluid in heat exchanger or in internal combustion chamber, this flow system may be highly participating to the radiation.

Therefore, in the case of seeding highly absorbing particles into the gas streams, the analysis for particle diffusion in non-isothermal gas neglecting the radiation effect for particle phase may result in significant error as Goren [6] pointed out. Furthermore, in a heat exchanger using the combustion exhaust gas in high temperature field, this effect should be taken into account. Nevertheless, as mentioned in the foregoing, no analysis of thermophoresis for the absorbing, emitting particles has been performed up to date except for only absorbing particles. Thus, the main purpose of present study is to analyse qualitatively the radiative effect on the thermophoretic particle transport when the highly absorbing, emitting particles are properly loaded in gas streams.

The present study is to be limited to one-way coupling situation; that is, the particle movement does not affect the gas flow. One-way coupling situation may be assumed when the particle mass loading is not high[7]. In this situation, all the governing equations of two phase flow system are not coupled in the numerical computation. In contrast, the radiation is coupled with the forced convection through the energy conservation equation which includes the divergence of radiative flux. Finally, in this work, the parametric study would be conducted using the dimensionless variables such as optical legnth τ_o and ratio of conduction to radiation N because of the deficiency of experimental data on the radiative properties.

GOVERNING EQUATIONS

The present study treats the dilute gas-particle flow that neglects the stress tensor (momentum transfer by diffusion) due to the infrequent interaction between the suspended particles(i.e $\tau_A/\tau_C<1$)[13]. And two fluid model would be used since it can be easily applied to the multi-dimensional flow system and also provides a rational frame work extendable to high mass loading. The theoretical analysis for thermophoresis phenomenon yields the following expression for the thermophoretic velocity.

$$v_T = -\frac{\nu K}{T}\nabla T \tag{1}$$

where K is the dimensionless thermophoretic coefficient and depends on the regime of flow past the particle described in terms of Knudsen number ($Kn=\lambda/(d_p/2)$) which represents the ratio of molecular mean free path to particle size. In transition regime where the molecular mean free path is on the order of the particle radius, Derjaguin et al.[3] give the following expression,

$$K=K_t\frac{1+C_t(\lambda/(d_p/2))(K_p/K_g)}{1+K_p/(2K_g)+C_t(\lambda/(d_p/2))(K_p/K_g)} \tag{2}$$

where, C_t is the temperature jump coefficient in the Smoluchowski formula and K_t is thermal slip coefficient. The values of these coefficients are 2.16 and 1.17 respectively.

They found a very good agreement with the experimental data with the numerical values of the thermophoretic coefficient K ranging from about 0.25 to 1.25 for the different types of aerosol particles.

For simplicity, the following assumptions are made in the present investigation.

1. Flow is a dilute gas-particle flow due to the low mass loading.
2. For the gas phase, the flow field is hydrodynamically fully developed and for particle phase, the same flow field is assumed to be used at the pipe inlet.
3. Temperature and particle concentration distributions are uniform at the pipe inlet.
4. Fluid and particle properties are independent of temperature.
5. Pipe wall is isothermal and gray.
6. The gas is transparent to radiation and the solids are limited to the gray absorbing, emitting particle without scattering.
7. The absorption coefficient is constant in all thermal field.
8. The effect of particle coagulation and collision is neglected.
9. The gas and particle phase are in the same temperature.

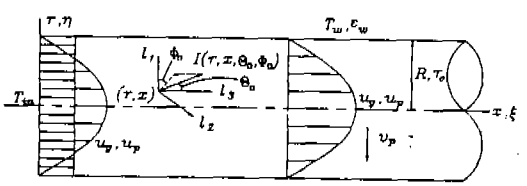

Fig. 1 Cylindrical coordinate system

The present problem configuration and coordinate system are depicted in Fig.1. On the basis of two fluid model, the governing equations of each phase can be written as follows:

Gas Phase

The gas phase velocity is assumed to be fully developed and is not altered by the particulate flow due to low mass loading. Hence the gas phase velocity may be expressed as

$$u_g = u_{max}\left[1 - \left(\frac{r}{R}\right)^2\right] \tag{3}$$

where,

$$u_{max} = 2U_{avg}$$

$$\rho_g C_{pg} v_g \cdot \nabla T_g = \nabla \cdot K_g \nabla T_g - \nabla \cdot q_g^R \tag{4}$$

Particle Phase

$$\nabla \cdot \rho_p v_p = 0 \tag{5}$$

$$\rho_p v_p \cdot \nabla v_p = -\rho_p \frac{v_p - v_g}{\tau_{mom}} - \rho_p \frac{\alpha_T D_p}{\tau_{mom}} \nabla \ln T_g \tag{6}$$

$$\rho_p C_{pp} \cdot \nabla T_p = -\rho_p C_{pp} \frac{T_p - T_g}{\tau_T} - \nabla \cdot q_p^R \tag{7}$$

where, τ_{mom} and τ_T are the momentum relaxation time and thermal relaxation time respectively.

Based on the above assumptions, the energy conservation equations(4) and (7) of each phase may be combined to the mixture energy equation form

$$\rho C_p v \cdot \nabla T = \nabla \cdot K_g \nabla T - \nabla \cdot q_p^R \tag{8}$$

where,

$$\rho C_p v = \rho_g C_{pg} v_g + \rho_p C_{pp} v_p$$

$$T = T_g \simeq T_p$$

For the particle phase, introducing the dimensionless variables, the equations(5) and (6) can be rewritten as

mass conservation

$$\frac{\partial}{\partial \xi}(\phi u_p) + \frac{1}{\eta}\frac{\partial}{\partial \eta}(\eta \phi v_p) = 0 \tag{9}$$

u - momentum

$$u_p \frac{\partial u_p}{\partial \xi} + v_p \frac{\partial u_p}{\partial \eta} = -\frac{1}{Stk}(u_p - u_g) - \frac{1}{Stk}\frac{K}{Re_R}\frac{1}{\theta}\frac{\partial \theta}{\partial \xi} \tag{10}$$

v - momentum

$$u_p\frac{\partial v_p}{\partial \xi}+v_p\frac{\partial v_p}{\partial \eta}=-\frac{1}{Stk}(v_p-v_g)-\frac{1}{Stk}\frac{K}{Re_R}\frac{1}{\theta}\frac{\partial \theta}{\partial \eta} \quad (11)$$

where,

$$\xi=\frac{x}{R},\quad \eta=\frac{r}{R},\quad u_p^*=\frac{u_p}{U_{avg}},\quad v_p^*=\frac{v_p}{U_{avg}}$$

$$\phi=\frac{\rho_p}{\rho_{p,in}},\quad \theta=\frac{T}{T_{in}},\quad Re_R=\frac{U_{avg}R}{\nu_g},\quad Stk=\frac{\tau_{mom}}{\tau_{flow}}$$

The superscript (*) is abbreviated hence-forth for convenience. The Stokes number is defined as the ratio of the momentum relaxation time(aerodynamic responce time) to the characteristic flow time(τ_{mom}/τ_{flow}) [13]. If the Stokes number is very small, the particles will move with the host fluid in the same manner. The similar concept can be applied to the thermal relaxation time and τ_{mom} coincides with τ_T when the Prandtl number is 2/3[14]. And also Pr=2/3 is used in the present calculation.

The boundary conditions for the above governing equations are taken as follows:

$$u_p=u_g,\quad v_p=0,\quad \phi=1 \qquad \text{at} \quad \xi=0$$

$$\frac{\partial u_p}{\partial \eta}=0,\quad V_p=0 \quad ,$$

$$\frac{\partial \phi}{\partial \eta}=0 \quad \text{(symmetry condition)} \quad \text{at} \quad \eta=0$$

Since the particle momentum equations are described by the first order partial differential equations, only the upstream boundary conditions are needed. Employing the following dimensionless quantities, equation(8) leads to

$$(1+C_L)v_g\cdot\nabla\theta=\frac{1}{Pe_R}\nabla^2\theta-\frac{1}{Bo}\nabla\cdot q_p^R \quad (12)$$

where,

$$C_L=\rho_pC_{pp}/\rho_gC_{pg},\ Pe_R=Re_RPr,$$

$$Bo=\frac{\rho_gC_{pg}U_{avg}}{4\sigma n^2T_{in}^3},\quad q_p^{*R}=\frac{q_p^R}{4\sigma n^2T_{in}^4}$$

Furthermore, for the absorbing and emitting medium, divergence of radiation flux is expressed by integrating the radiative transfter equation over a solid angle 4π as follows [15, 16]:

$$\nabla\cdot q_p^R=[4\pi I_b-I_o] \quad (13)$$

where, the details of I_o would be described in the following section.

Rewriting the equation(12) using the above expression in the dimensionless form,

$$(1+C_L)\left(u_g\frac{\partial\theta}{\partial\xi}+v_g\frac{\partial\theta}{\partial\eta}\right)=\frac{1}{Pe_R}\frac{\partial^2\theta}{\partial\xi^2} \quad (14)$$

$$+\frac{1}{Pe_R}\frac{1}{\eta}\frac{\partial}{\partial\eta}\left(\eta\frac{\partial\theta}{\partial\eta}\right)-\frac{\tau_o^2}{Pe_R\,N}(\theta^4-G_o)$$

where,

$$\tau_o=\beta R,\quad N=\frac{K_g\beta}{4\sigma n^2T_{in}^3}$$

$$G_o=\frac{I_o}{4\sigma n^2T_{in}^4}$$

subject to the boundary conditions,

$$\theta=1 \qquad \text{at} \quad \xi=0$$

$$\frac{\partial^2\theta}{\partial\xi^2}=0 \qquad \text{at exit}$$

$$\frac{\partial\theta}{\partial\eta}=0 \qquad \text{at} \quad \eta=0$$

$$\theta=\theta_w \qquad \text{at} \quad \eta=1$$

And coefficient C_L is assumed to be in the range less than 0.2 under the assumption of low mass loading and proper heat capacity for the particle phase.

The particle deposition flux to the wall may be expressed as

$$J_p=\phi v_p|_w \quad (15)$$

Also, the cumulative collection efficiency is defined as the percentage of the particles

that are deposited on the wall within a distance x from the tube inlet.

$$E(x)=\frac{\int_0^x J_p(s)2\pi\, ds}{\phi_{in}U_{avg}\pi R} \tag{16}$$

RADIATION MODEL

When a participating medium is present, the mathematical complexity increases considerably in the formulation of energy equation due to the nonlinear integral nature and the fourth order temperature dependence of radiative transfer.

In this study, in order to simplify the analysis, P-1 approximation(spherical harmonics method) which is one of the differential approximation methods is to be taken [17,18, 19,20,21]. Under consideration of the radiative heat transfer for absorbing, emitting medium neglecting the scattering effect in the axisymmetric circular cylinder(see Fig.1 for the formulation of radiation), the radiative transfer equation is as follows[17];

$$\left[\frac{1}{\beta}\left(l_1\frac{\partial}{\partial r}-\frac{1}{r}l_2\frac{\partial}{\partial\phi_\Omega}+l_3\frac{\partial}{\partial x}\right)+1\right]I(r,x,\theta_\Omega,\phi_\Omega)=I_b \tag{17}$$

where, l_1, l_2, l_3 are direction cosines

$$l_1=\cos(\phi_\Omega)\sin(\theta_\Omega)$$

$$l_2=\sin(\phi_\Omega)\cos(\theta_\Omega)$$

$$l_3=\cos(\theta_\Omega)$$

Applying P-1 approximation to equation (17), the following equation for the non-scattering gray medium can be obtained[17],

$$\left(\frac{\partial^2}{\partial\eta^2}+\frac{1}{\eta}\frac{\partial}{\partial\eta}+\frac{\partial^2}{\partial\xi^2}\right)I_o=3(I_o-4\pi I_b)\tau_o^2 \tag{18}$$

where,

$$I_o(r,x)=\int_{4\pi}I(r,x,\Omega)\,d\Omega$$

For the boundary condition, Marshak's condition is adopted since Marshak's is preferable to Mark's for lower order approximation[15]. The resulting boundary conditions are as follows[19]:

$$I_o\pm E_i\frac{\partial I_o}{\partial z}=4\pi I_{bw,i} \tag{19}$$

where,

$$E_i=2(2-\epsilon_{wi})/3\beta\epsilon_{wi},\quad z=r,x\quad;\quad i=1,2$$

The minus sign is corresponding to the lower boundary and plus sign to the upper boundary and ϵ_w is taken as 0.7 in the present calculation.

RESULTS AND DISCUSSION

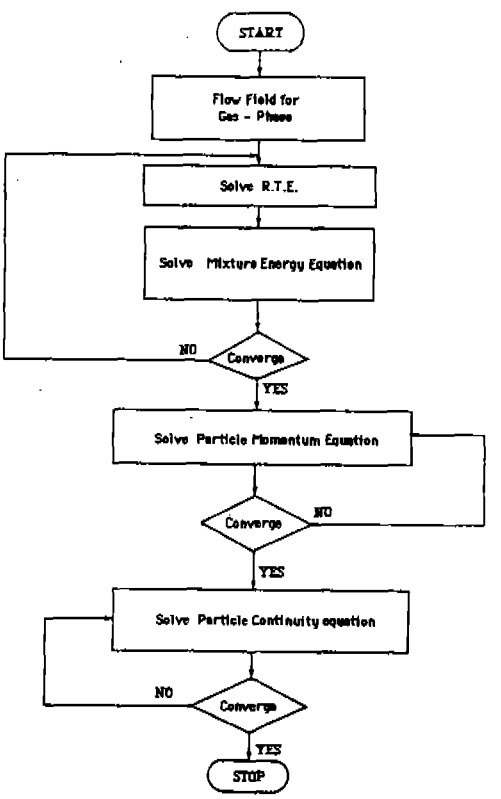

Fig. 2 Flow Chart for Numerical Calculation

The approximate layout for the present numerical calculation procedure is refered to Fig.2. First, in order to check the accuracy of the present numerical method, the results are compared with the solutions by Walker et al.[10] and Pearce and Emery[22]. As shown in Fig.3, in the absence of radiation, the present results of the cumulative collection efficiency due to the thermophoretic paticle transport are in a good agreement with Walker's results by trajectory model for the particle species conservation equation.

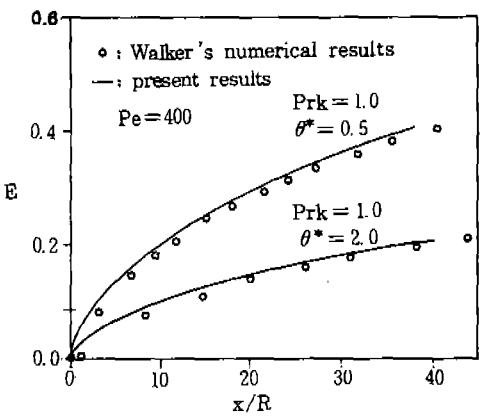

Fig. 3 Cumulative collection efficiency along axial distance for different operating conditions

Figure 4 shows that P-1 approximation solution for the coupled energy equation involving the radiative flux give a good agreement comparing to the Pearce and Emery's results. In the following figures, the solutions are presented in terms of the optical radius τ_o and conduction-to-radiation parameter N which are the most typical ones characterizing radiative heat transfer.

In Fig.5, the mixed mean temperature distributions along axial distance are depicted with the varition of τ_o at N=0.01. Because of the nonlinear source term in equations(14), the solution procedures are of iterative nature and EL2D code developed by Patankar was

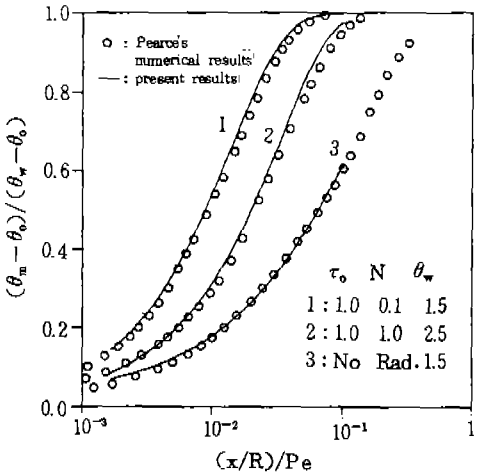

Fig. 4 Mean temperature vs. (x/R)/Pe

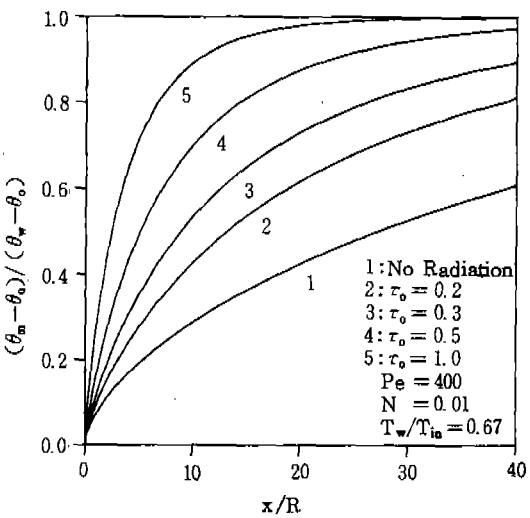

Fig. 5 Mean temperature along axial distance (effect of τ_o)

used. In particular, with the increase in τ_o, the mean temperature approaches asymptotically to the wall temperature more rapidly due to the increased radiative heat loss to the wall. Hence the thermal entry length is expected to become shorter.

Figure 6 shows the effect of radiation with the variation of τ_o on the particle diffusion velocity in the case of T_w/T_{in}=0.67, θ*=2.0. This drift velocity is dominated by the fully known source term in the momentum equa-

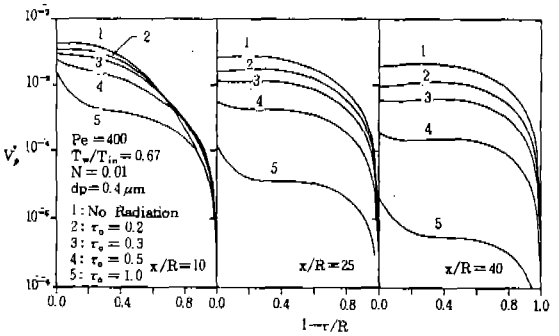

Fig. 6 Particle diffusion velocity profiles at arbitrary axial distances (effect of τ_o)

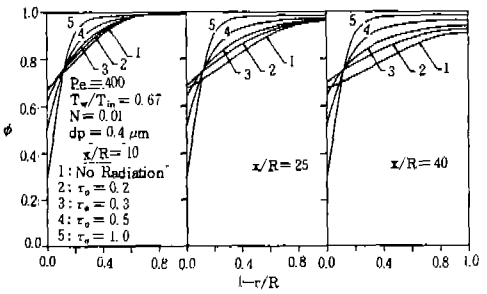

Fig. 7 Particle concentration profiles at arbitrary axial distances (effect of τ_o)

tions of particle phase which are solved using upwind scheme. As expressed in the equations (1) and (2), its diffusion velocity is strongly dependent upon the Knudsen number in relation with the particle size and temperature gradient. The thermophoretic coefficient K from Derjaguin's expression may be obtained under the condition of d_p=0.4 μm in submicron size neglecting the inertial transport mechanism. At τ_o=0, as moving downstream, the particle diffusion velocity decreases slightly near the wall, while increasing far from the wall. With the increase in the optical radius τ_o, near the entrance region(x/R=10), the radial component V_p* becomes slightly larger than that of τ_o=O in the tube core region. When the radiation is neglected, heat transfer occurs only through diffusion process and hence the thermal boundary layer is confined in the vicinity of the wall. However, when the radiation is present, due to the far reaching nature, the temperature gradient may exist even in the core region. In addition, in the case of strong radiation (τ_o=1.0), there is no particle transport in the core region since the temperature profile becomes flat except in the conduction region near the wall.

Figure 7 gives a series of concentration profiles at three axial distances, x/R=10, x/R=25, x/R=40 for various optical radii at T_w/T_{in}=0.67, N=0.01. As shown, near the wall surface, the particle concentration is abruptly decreased with the increase in τ_o. It follows that the concentration boundary layer becomes thinner. Along axial distance, the difference in the particle concentration between the various τ_o's is increased except the conduction region as expected from Fig.6. In addition, for smaller τ_o, the concentration ϕ tends to decrease along axial distance because of the cumulative deposition to the wall by the thermophoretic effect until the fluid temperature equilibrates with the wall temperature over x/R=40. Thus, much more difference in ϕ between the τ_o's would be expected.

In fact, higher overall particle concentration over the tube cross-section except for the vicinity of wall is illustrated for larger effect of radiation. As shown in Fig.7, since the particle concentration distribution is not distributed uniformly for various τ_o, the present assumption of uniform absorption coefficient in all thermal field may not be valid. However, this assumption is considered to be sufficient to investigate the qualitative trend while avoiding the complexity involving the concentration dependence on radiative property.

Figure 8 shows the effect of τ_o and N for the cumulative collection efficiency E(x) along axial distance. The thermophoretic

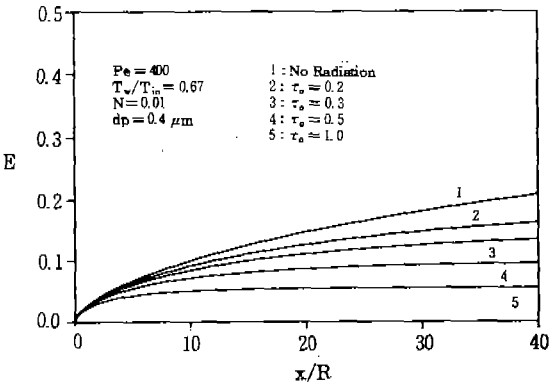

Fig. 8 Cumulative collection efficiency along axial distance(effect of τ_0)

particle flux can be obtained from the particle diffusion velocity and concentration at the wall. With the increase in τ_0, E(X) reaches more quickly to some constant value asymptotically. At x/R=40, the cumulative collection efficiency for larger τ_0 is considerably low compared with that of 'no radiation'. It would be expected much lower in the further downstream region. In gas-solid suspension flow system, it is desirable to enlarge the hydraulic radius and mass loading ratio even for the weakly radiating medium and to employ the particulate materials with high surface emissivity in order to have low E(x) as prescribed in absorption coefficient $\beta=\pi(d_p/2)^2 n_p \epsilon_p$.

Figure 9 illustrates the effect of τ_0 and T_w/T_{in} on the cumulative collection efficiency at x/R=40. As mentioned earlier, it is indicated that the increase of τ_0 and decrease of T_w/T_{in} result in higher efficiency. When the strong radiative effect over τ_0=0.5 is applied to thermophoresis phenomenon, the rate of increase in the efficiency for decreasing T_w/T_{in} becomes lower than that without radiation effect.

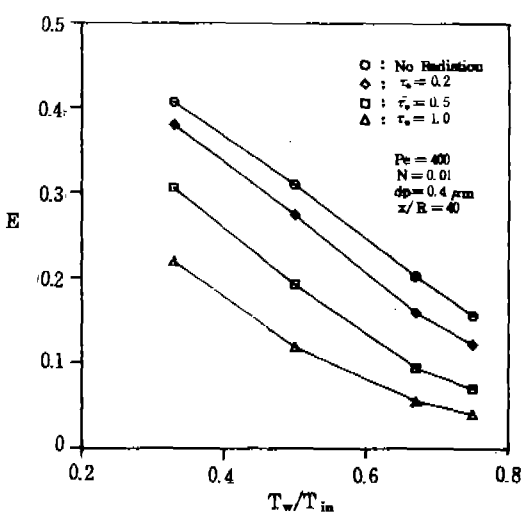

Fig. 9 Cumulative collection efficiency vs. T_w/T_{in} for various τ_0

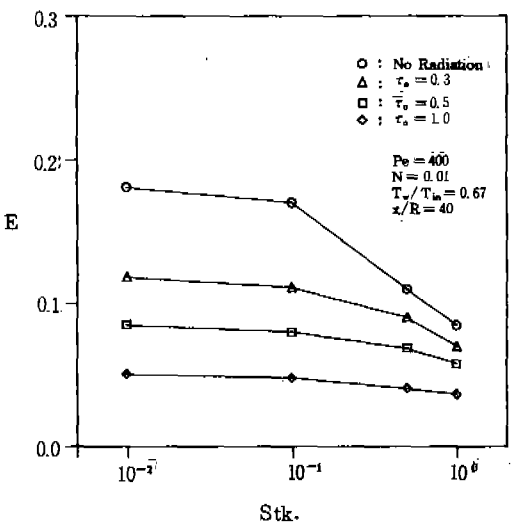

Fig. 10 Cumulative collection efficiency vs. Stokes number for various τ_0

Figure 10 shows the effect of the Stokes number on the efficiency E(x). Particularly, in this figure, the variation of the Stokes numbers for constant particle size (d_p=1μm) is considered in spite of strong dependence of Stk on the particle size. From this figure, it is noted that the decrease in efficiency is to be taken over Stk=0.1 in all cases. In the case of 'no radiation', very sudden drop in the efficiency E(x) is shown at Stk=0.1, while a gradual decrease is suggested for larger τ_0. In particular, for larger τ_0, smaller rate of the

decrease in efficiency E(x) is illustrated. It is also notable that for τ_0=1.0, the efficiency remains nearly constant. Moreover, in parallel gas streams, with the increase in the Stokes number causing the inertial transport mechanism for large particles under consideration of the scattering effect, a similar trend for the cumulative collection efficiency may be expected within the proper limitation to particle size from this figure.

CONCLUSION

In a non-isothermal field, thermophoresis is a dominant mechanism for the particle diffusion in the range of the low Stokes numbers. Several important observations are noted and summarized below. In the absence of confirming experimental evidence, the observations are mainly of qualitative value.

1. When the strong radiative contribution is included, the concentration boundary layer becomes thin due to much smaller value of the particle diffusion velocity far from the wall compared to that without radiation.
2. As expected from the particle concentration and drift velocity distribution, the cumulative collection efficiency becomes considerably lower when the highly absorbing, emitting material is present under the proper loading condition.
3. As the ratio of wall to inlet gas temperature causing the change of thermal field is decreased, the difference of the cumulative collection efficiency between τ_0's is notably increased at $\tau_0 \geq 0.5$.
4. At the critical Stokes number(=0.1), the rate of decrease for the efficiency E(x) becomes larger; that is, due to the inertial transport mechanism in parallel flow system, the thermophoretic effect is reduced in the deposition of particles to the cold wall. Moreover, this behaviour becomes significant in the absence of the radiation, while less important as the radiative effect increases.

REFERENCES

1. Batchelor G.K. and Shen C. 'Thermophoretic Deposition of Particles in Gas Flowing over Cold Surfaces' *J. Colloid and Interface Science, 1985,* **107**(1), 21-36.
2. Fulford G.D., Moo-Young M. and Bebu M. 'Thermophoretic acceleration of particle deposition from laminar air streams' *Canad. J. Chem. Eng., 1971,* **49**, 553-556.
3. Derjaguin B.V., Rabinovich Ya. I., Storzhilova A.I. and Shcherbina G.I. 'Measurement of the coefficient of thermal slip of gases and the thermophoresis velocity of large-size aerosol particales' *J. Colloid and Interface Science, 1976,* **57**, 451-461.
4. Goldsmith P. and May F.G. Aerosol Science, *Acadmic Press, New York, 1966.*
5. Rosner D.E. and Kim S.S. 'Optical experiments on thermophoretically augmented submicron particle deposition from 'Dusty' high temperature gas flows' *Chem. Eng. J., 1984,* **29**.
6. Goren S.L. 'Thermophoresis of aerosol particles in the laminar boundary layer on a flat plate' *J. Colloid and Interface Science, 1977,* **61**(1), 77-85.
7. Lee J.S. and Humphrey J.A.C. 'Radiative-convective heat transfer in dilute particle-laden channel Flows' *Physico Chemical Hydrodynamics, 1986,* **7**(5/6), 325-351.
8. Calvert S. and Byers L.J. *Air Pollution Control Assoc., 1967,* **17**, 595.
9. Epstein M., Hauser G.M. and Henry R.E. 'Thermophoretic deposition of particles in natural convection flow a vertical plate' *ASME, J. Heat Transfer, 1985,* **107**,

272-276.

10. Walker K.L., Homsy G.M. and Geyling F.T. 'Thermophoretic deposition of small particles in laminar tube Flow' *J. Colloid and Interface Science, 1979,* **69**(1), 138-147.
11. Morse T.F., Wang C.Y. and Cipolla, Jr J.W. 'Laser-induced thermophoresis and particulate deposition efficiency' *ASME, J. Heat Transfer, 1985,* **107**, 155-160.
12. Cipolla, Jr J.W. and Morse T.F. 'Thermophoresis in an absorbing aerosol' *J. Aerosol Science, 1987,* **18**(3), 245-260.
13. Crowe C.T. 'Review-numerical methods for dilute gas-particle flow' *ASME, J. Fluids Engineering, September 1982,* **104**, 297-303.
14. Marble F.E. 'Dynamics of dusty gases' *Ann. Review, Fluid Mech., 1970,* **2**, 397-446.
15. Ozisik M.N. Radiative Transfer. *John Wiley, 1973.*
16. Siegel R. and Howell J.R. 'Thermal Radiation Heat Transfer. *McGraw-Hill, New York, 1972.*
17. Menguc M.P. and Viskanta R. 'Radiative transfer in exisymmetric finite cylindrical enclosures' *ASME, J. Heat Transfer, May 1986,* **108**, 271-276.
18. Menguc M.P. 'Modeling of radiative heat transfer in multidemensional enclosures using spherical harmonics approximation' *Ph.D. Thesis, Purdue University, 1986.*
19. Higenyi J. and Bayazitoglu Y. 'Differential approximation of radiative heat transfer in a gray medium' *ASME, J. Heat Transfer, November 1980,* **102**, 719-723.
20. Heaslet M.C. and Warming R.F. 'Theoretical predictions of radiative transfer in a homogeneous cylindrical medium' *J. Quan. Spec. and Rad. Tran., 1966,* **6**, 751-774.
21. Desoto S. 'Coupled radiation, conduction and convection in entrance flow' *Int. J. Heat and Mass Transfer, 1975,* **11**, 245-259.
22. Pearce B.E. and Emery A.F. 'Heat transfer by thermal radiation and laminar forced convection to an absorbing fluid in the entry region of a pipe' *ASME, J. Heat Transfer, May 1970,* **92C**, 221-230.